

Phonon instabilities in bcc Sc, Ti, La, and Hf

Kristin Persson and Mathias Ekman

Theoretical Physics, Royal Institute of Technology, SE-100 44 Stockholm, Sweden

Vidvuds Ozoliņš

Sandia National Laboratories, P.O. Box 969, Livermore, California 94551-0969

(Received 18 January 2000)

The lattice dynamics of the elements Sc, Ti, La, and Hf in the bcc structure is studied using the density-functional linear-response theory. The elements exhibit similar phonon instabilities which cover large parts of the Brillouin zone. In particular, the entire $T_{[1\bar{1}0]}[\xi\xi0]$ branch, where the zone-boundary phonon is responsible for the bcc→hcp transition, and the $L[\frac{2}{3}\frac{2}{3}\frac{2}{3}]$ mode (bcc→omega) are unstable. However, the $T[\xi\xi\xi]$ branch is unstable for all elements except Sc, and Ti and Sc exhibit distorted bcc energy minima not seen in the other elements.

There is a series of early transition-metal elements (Sc, Ti, Y, Zr, La, Hf) exhibiting a low-temperature close-packed phase and a high-temperature bcc phase. Measured phonon dispersions for these elements in the bcc phase are dominated by low-energy phonon modes interpreted as structural phase-transition precursors.¹⁻⁵

The stability of the high-temperature phase has been attributed to the vibrational excess entropy of these low-energy phonons. First-principles total-energy studies⁶ of a few high-symmetry phonons in bcc Zr have revealed that some phonon modes are not only soft but even dynamically unstable at $T=0$ K. It has been suggested that anharmonic effects stabilize these modes at high temperatures. However, the exact mechanism of this high-temperature stabilization is still uncertain. Classical⁷ and tight-binding⁸ molecular-dynamics simulations can provide some insights into the anharmonic dynamics of these systems, although they are often hampered by the accuracy of the underlying force-field model. For instance, it is important that the employed potential models reproduce all $T=0$ K dynamical instabilities and structural energy differences.

In the present work we perform systematic first-principles phonon-dispersion calculations for the bcc structures of four representative elements which all exhibit a high-temperature bcc phase: Sc, Ti, and Hf which are hexagonal close-packed and La which is double hexagonal close-packed at low temperature. Our results can be used not only to assess the accuracy of potential models in molecular-dynamics simulations, but also in the more general context of understanding lattice instabilities. In particular, dynamical phonon instabilities are often discussed in terms of transformation paths to energetically more stable high-symmetry structures. Such studies usually concentrate on particular well-known transition paths and corresponding phonon modes and thus may miss unsuspected instabilities. By systematically calculating the complete phonon dispersions we can probe deeper into the nature of dynamical instabilities and reveal new unstable modes that are not directly related to any known structural transformation paths.

We use density-functional theory⁹ in the local-density approximation (LDA).¹⁰ The phonon frequencies are calculated using the density-functional linear-response method.¹¹⁻¹³ The calculations are performed using a plane-wave basis set

and norm-conserving pseudopotentials.¹⁴ Extended s and p semicore states of Sc, Ti, La, and Hf are treated as valence states. The f bands in La and Hf are not included. Previous calculations of the lattice dynamics and equilibrium properties in fcc La (Ref. 15) have found that the effects due to the almost empty $4f$ bands are rather small. The core radii are chosen to be between 2.4 and 2.6 a.u. This scheme allows for a total-energy convergence better than 0.2 mRy/atom for cut-off energies $E_{\text{cut}}=30$ Ry for La and Hf and $E_{\text{cut}}=40$ Ry for Ti and Sc. The Brillouin-zone summations are carried out on a $16\times 16\times 16$ Monkhorst-Pack¹⁶ grid and the electronic states are populated according to Fermi-Dirac statistics with $T=1272$ K which is representative of the temperature where the studied elements are experimentally observed in the bcc phase (Sc:1608 K, Ti:1155 K, La:1134 K, Hf:2016 K).¹⁷

Table I shows the calculated and measured values for equilibrium lattice parameters and bulk moduli, which can be used to estimate both the accuracy of our pseudopotentials and the local-density approximation for the studied systems. Comparison of pseudopotential (PP) and full-potential linear-augmented-plane-wave¹⁸ (FP-LAPW) results demonstrates that the inaccuracies introduced by the PP approximation are negligible. However, both PP and FP-LAPW equilibrium lattice parameters are too low in comparison with the experimental values, which can be attributed to the well-known overbinding phenomena of LDA.^{19,20} This overbinding leads to calculated elastic constants (cf. Table II) and phonon frequencies (cf. Table III) that are usually higher by 10–20% than the experimental values. Having established the accuracy of the LDA and of the constructed pseudopo-

TABLE I. Equilibrium lattice parameters and bulk moduli for the $T=0$ K stable phases of Sc, Ti, La, and Hf.

| Element | Struc. | a (a.u.) | | | B (Mbar) | | |
|---------|--------|------------|------|-------|------------|------|-------|
| | | PP | LAPW | Expt. | PP | LAPW | Expt. |
| Sc | hcp | 6.01 | 6.05 | 6.25 | 0.59 | 0.61 | 0.44 |
| Ti | hcp | 5.39 | 5.41 | 5.57 | 1.33 | 1.25 | 1.05 |
| La | dhcp | 7.00 | 6.83 | 7.12 | 0.33 | 0.32 | 0.24 |
| Hf | hcp | 5.87 | 5.88 | 6.04 | 1.19 | 1.20 | 1.09 |

TABLE II. Calculated elastic constants for bcc Sc, Ti, La and Hf (upper table) and linear combinations of the elastic constants to which the acoustic velocities ($v^2 \propto \sum a_{ij} C_{ij}$) are related for the different high-symmetry branches in a cubic structure (lower table).

| Element | C_{11} (Mbar) | C_{12} (Mbar) | C_{44} (Mbar) |
|-----------------|----------------------------|----------------------------|------------------------------|
| Sc | 0.4 | 0.6 | 0.3 |
| Ti | 1.2 | 1.4 | 0.2 |
| La | 0.0 | 0.5 | 0.1 |
| Hf | 0.9 | 1.3 | 0.4 |
| Branch | T_1 | T_2 | L |
| $[\xi 00]$ | C_{44} | C_{44} | C_{11} |
| $[\xi \xi 0]$ | $C_{11} - C_{12}$ | $2C_{44}$ | $C_{11} + C_{12} + 2C_{44}$ |
| $[\xi \xi \xi]$ | $C_{11} - C_{12} + C_{44}$ | $C_{11} - C_{12} + C_{44}$ | $C_{11} + 2C_{12} + 4C_{44}$ |

entials for Sc, Ti, La, and Hf, we proceed to study dynamical properties of the bcc structures of these elements.

Figure 1 presents the calculated phonon dispersion curves $\nu(\mathbf{q})$ for bcc Sc, Ti, La, and Hf at their respective equilibrium volumes where $-|\nu|$ is plotted when $\nu^2(\mathbf{q}) < 0$. A third-order spline is used to interpolate between the directly calculated frequencies. In Fig. 2 we show a few select phonon branches scaled to the H -point phonon frequency value, to illustrate the most interesting similarities and differences between the elements.

The elastic constant $C' = \frac{1}{2}(C_{11} - C_{12})$, manifested in the long-wavelength part of the transverse branch along $[\xi \xi 0]$ with the polarization vector along $[1\bar{1}0]$ (cf. Table II), is negative. This implies an instability towards the fcc structure through Bain's path. Figure 3 presents the trigonal and tetragonal distortions²⁴ of the bcc structure for all the elements in this study. There is a metastable (with respect to C' distortions) tetragonal structure around $c/a = 0.84$ for Ti, Hf, and La but not for Sc, which exhibits a shallower minimum at $c/a = 0.92$. A shearing of the bcc crystal into $c/a = 0.84$ corresponds very well to the transformation of $(110)_{bcc}$ planes into $(001)_{hcp}$ planes. Since the bcc crystal needs to be sheared to $c/a = 0.816$ to reach the hcp phase we conclude that this motion in Sc has to take place simultaneously with (or after) the distortion corresponding to the $T_{[1\bar{1}0]}[\frac{1}{2}\frac{1}{2}0]$ phonon mode.

The entire transverse $[\xi \xi 0]$ branch with polarization along $[1\bar{1}0]$ is unstable. The zone-boundary mode of this branch, $T_{[1\bar{1}0]}[\frac{1}{2}\frac{1}{2}0]$, has been studied in several

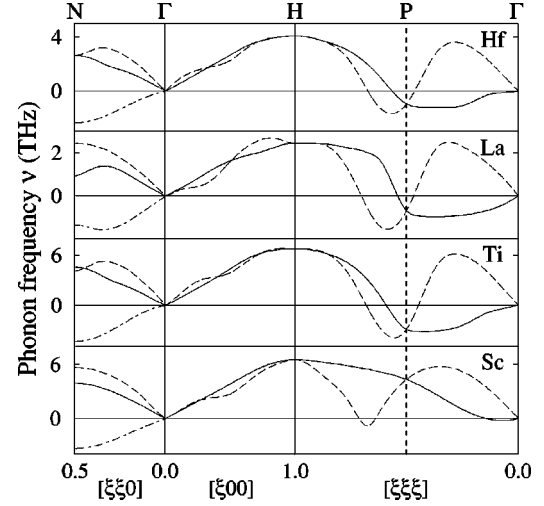


FIG. 1. Calculated phonon frequencies of bcc Sc, Ti, La, and Hf. The longitudinal branch is the dashed lines and the transverse branches are solid lines except for the $[1\bar{1}0]$ polarization in the $[\xi \xi 0]$ direction which is dot dashed.

systems,^{25–28} since it, together with an elastic strain associated with C' , gives a possible path for the martensitic bcc to hcp transformations.

We observe that the $T_{[1\bar{1}0]}[\frac{1}{4}\frac{1}{4}0]$ phonon mode provides a transition path (together with C') from the bcc to the dhcp structure. A pressure-induced softening for this mode in W has been noted in an earlier first-principles work.²⁹ The $T_{[1\bar{1}0]}[\frac{1}{3}\frac{1}{3}0]$ phonon transforms (together with C' and a tilt of the bcc $[110]$ axis) the bcc structure to the $9R$ structure. This mode has been studied primarily in Li and Na,^{30,31} which both show a low-temperature transformation from bcc to $9R$. In Fig. 2 we see a marked difference between the $T_{[1\bar{1}0]}[\xi \xi 0]$ branch in La compared to the other elements. In lanthanum, which is double hexagonal close packed at low temperatures, the minimum of the $T_{[1\bar{1}0]}[\xi \xi 0]$ branch is positioned well before the zone boundary. This is due to a steeper phonon instability towards the dhcp and $9R$ structures than to the hcp structure. However, the path to all these structures include a C' distortion and in the case of $9R$ a tilt as well as C' , which makes it difficult to draw conclusions about the relative stability of the phases from small differences in the phonon frequency. Total-energy calculations for La at zero temperature reveal that $9R$ is 0.7 mRy/atom above the dhcp structure.

A broad instability occurs around the $L[\frac{2}{3}\frac{2}{3}\frac{2}{3}]$ mode. This

TABLE III. Experimental and calculated phonon frequencies for hcp Sc, Ti, and Hf at the M point.

| | Work | ν (THz) | | | | | |
|----|-----------------|------------------|--------------|--------------|------------------|------|------|
| | | TA_{\parallel} | TA_{\perp} | TO_{\perp} | TO_{\parallel} | LA | LO |
| Sc | Calc. | 3.66 | 4.18 | 6.71 | 6.43 | 5.79 | 6.57 |
| | Expt. (Ref. 21) | 3.57 | 3.97 | 6.23 | 6.11 | 6.21 | 6.23 |
| Ti | Calc. | 3.52 | 3.46 | 6.84 | 7.09 | 8.16 | 8.50 |
| | Expt. (Ref. 22) | 3.4 | 3.82 | 6.06 | 6.95 | 7.1 | 7.69 |
| Hf | Calc. | 1.95 | 2.16 | 3.72 | 3.70 | 4.26 | 4.30 |
| | Expt. (Ref. 23) | 2.08 | 2.35 | 3.5 | 3.62 | 3.85 | 4.3 |

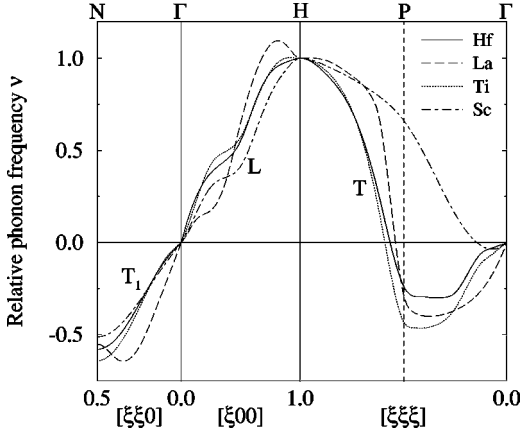


FIG. 2. Relative phonon frequencies for selected branches of bcc Sc, Ti, La, and Hf scaled to the H -point value. The $T_{1[\xi\xi 0]}$ branch has the polarization vector $[1\bar{1}0]$.

mode has been studied extensively^{6,25,32} from first principles, particularly in bcc Zr where it was found to be unstable at zero temperature. Experiments at high temperatures for the elements in this study all show a pronounced softening at $\mathbf{q} = [\frac{2}{3}\frac{2}{3}\frac{2}{3}]$ for the longitudinal mode.¹⁻⁴ It has been argued that the weakness towards the ω structure in these elements should be seen as an intrinsic property. It is also important to point out that the minimum of the longitudinal branch is *not* positioned at $\xi = \frac{2}{3}$ but rather at $\xi = \frac{7}{12}$ for all elements except Sc.

The $[\xi 00]$ direction shows an anomalous crossing of the longitudinal and the transverse branch which is not observed experimentally in the high-temperature bcc phases of early transition metals, suggesting that it is most likely suppressed by strong anharmonic effects. In Nb, this anomaly is seen at ambient conditions but vanishes at high temperatures³³ and is explained as a consequence of the highly anisotropic Fermi surface.³⁴ From Fig. 2 we note that the anomalous crossing is remarkably similar for all elements except for La.

A large part of the transverse $[\xi\xi\xi]$ branch is unstable for

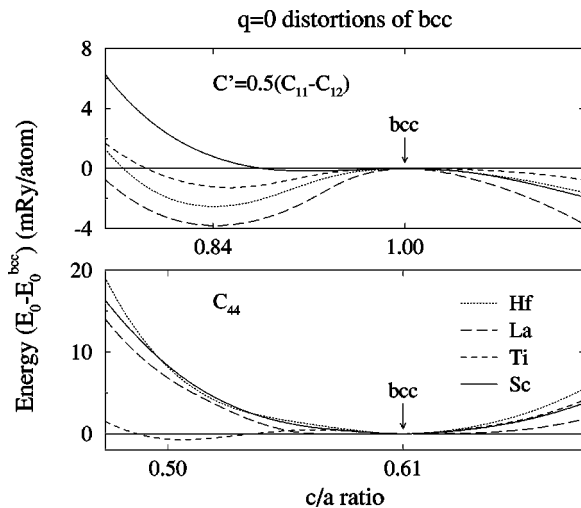


FIG. 3. Energy for distortions of the bcc structure corresponding to the elastic constants C' (upper panel) and C_{44} (lower panel). Note that the c/a ratios refer to different axes for the two distortions (Ref. 24).

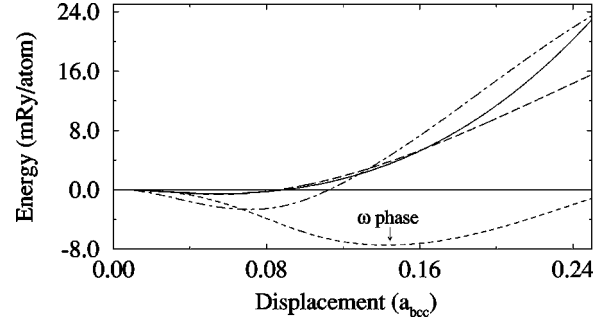


FIG. 4. Energy for distortions of the bcc structure in Ti corresponding to the $T_{1[\bar{1}\bar{1}0][\frac{1}{3}\frac{1}{3}\frac{1}{3}]}$ (long-dashed), $T_{1[112][\frac{1}{3}\frac{1}{3}\frac{1}{3}]}$ (solid), $T_{1[\bar{1}\bar{1}0][\frac{1}{2}\frac{1}{2}0]}$ (dot-dashed), and $L[\frac{2}{3}\frac{2}{3}\frac{2}{3}]$ (dashed) phonons.

Ti, La, and Hf which is surprising since experiments show no anomalous damping of this branch. This is also a significant difference between the elements in the study since this instability is not present in Sc, cf. Fig. 2. To study the instability of the $T[\xi\xi\xi]$ branch we performed frozen-phonon calculations for two phonons in the beginning and the end of the most unstable region, i.e., $\mathbf{q} = [\frac{1}{3}\frac{1}{3}\frac{1}{3}]$ and $\mathbf{q} = [\frac{1}{2}\frac{1}{2}\frac{1}{2}]$. Figure 4 shows the energy for distortions corresponding to the modes $T_{1[\bar{1}\bar{1}0][\frac{1}{3}\frac{1}{3}\frac{1}{3}]}$ and the $T_{1[112][\frac{1}{3}\frac{1}{3}\frac{1}{3}]}$ in Ti which are representative of the behavior of the $T[\xi\xi\xi]$ branch phonons we have studied. Also, for comparison, we include the results for the $T_{1[\bar{1}\bar{1}0][\frac{1}{2}\frac{1}{2}0]}$ and the $L[\frac{2}{3}\frac{2}{3}\frac{2}{3}]$ modes. The minima for the $T[\frac{1}{3}\frac{1}{3}\frac{1}{3}]$ phonons are very shallow which suggests that these phonons alone do not provide a path to a significantly more stable structure. The simplest explanation for the broad instability of the transverse branch is that it results from the combination of the instability in the $q \rightarrow 0$ limit, due to negative value of $C_{11} - C_{12} + C_{44}$ (cf. Table II), and the degeneracy of the transverse and longitudinal branch at $q = [\frac{1}{2}\frac{1}{2}\frac{1}{2}]$.

The long-wavelength $T_{1[001][\xi 00]}$ modes, corresponding to C_{44} (cf. Table II and the lower panel of Fig. 3), are stable. From Fig. 3 we also observe that Ti has an additional minimum at $c/a = 0.51$. We performed linear-response calculations for Ti at the trigonal distortion $c/a = 0.51$, which showed that the $T_{1[\bar{1}\bar{1}0][\xi\xi 0]}$ and $L[\xi\xi\xi]$ branches still exhibited deep instabilities, but the $T[\xi\xi\xi]$ branch was stabilized except for a sharp instability at $\xi = \frac{1}{3}$. This also suggests that the $T[\xi\xi\xi]$ branch is strongly coupled to other distortions and may be stabilized at low temperatures by the atomic motions. This would explain why no softening of this branch is seen in experiments.

In conclusion, we have calculated the phonon dispersions for four representative elements in their high-temperature bcc structure. Instabilities occur in large parts of the zone and are common to all elements except for a broad instability of the $T[\xi\xi\xi]$ branch, which is not seen in Sc. The $L[\xi 00]$ branch exhibit phonon anomalies which are almost identical in Ti, Sc, and Hf, but slightly different in La. These have not been seen in experiments. It is also interesting to note the differences in the energy surface around the bcc structure. All elements except Sc have pronounced minimum at $c/a \approx 0.84$, which corresponds very well to the shearing of the bcc planes into hexagonal ones. The distortion corresponding

to the elastic constant C_{44} yields in Ti a minimum, not present in the other elements.

K.P. and M.E. were supported by the Swedish research councils SSF. Most of the calculations were performed at the

Swedish primary national resource for high-performance computing and networking, Paralleldatorcentrum - PDC. V.O. was supported by the office of Basic Energy Science, Division of Materials Science, of the U.S. Department of Energy under Contract No. DE-AC04-94AL85000.

-
- ¹W. Petry, A. Heiming, J. Trampenau, M. Alba, C. Herzig, H. R. Schober, and G. Vogl, *Phys. Rev. B* **43**, 10 933 (1991).
- ²J. Trampenau, A. Heiming, W. Petry, M. Alba, C. Herzig, W. Miekeley, and H. R. Schober, *Phys. Rev. B* **43**, 10 963 (1991).
- ³F. Güthoff, W. Petry, C. Strassis, A. Heiming, B. Hennion, C. Herzig, and J. Trampenau, *Phys. Rev. B* **47**, 2563 (1993).
- ⁴W. Petry, J. Trampenau, and C. Herzig, *Phys. Rev. B* **48**, 881 (1993).
- ⁵A. Heiming, W. Petry, J. Trampenau, M. Alba, C. Herzig, H. R. Schober, and G. Vogl, *Phys. Rev. B* **43**, 10 948 (1991).
- ⁶Y. Chen, C.-L. Fu, K. M. Ho, and B. N. Harmon, *Phys. Rev. B* **31**, 6775 (1985).
- ⁷B. L. Zhang, C. Z. Wang, K. M. Ho, D. Turner, and Y. Y. Ye, *Phys. Rev. Lett.* **74**, 1375 (1995).
- ⁸H. Haas, C. Z. Wang, K. M. Ho, M. Fähnle, and C. Elässer, *J. Phys.: Condens. Matter* **11**, 5455 (1999).
- ⁹P. Hohenberg and W. Kohn, *Phys. Rev.* **136**, A864 (1964); W. Kohn and L. J. Sham, *ibid.* **136**, A1133 (1965).
- ¹⁰D. M. Ceperley and B. J. Alder, *Phys. Rev. Lett.* **45**, 566 (1980); J. P. Perdew and A. Zunger, *Phys. Rev. B* **23**, 5048 (1981).
- ¹¹S. Baroni, P. Giannozzi, and A. Testa, *Phys. Rev. Lett.* **58**, 1861 (1987); P. Giannozzi, S. de Gironcoli, P. Pavone, and S. Baroni, *Phys. Rev. B* **43**, 7231 (1991).
- ¹²V. Ozoliņš, Ph.D. thesis, Royal Institute of Technology, Sweden, 1996.
- ¹³S. de Gironcoli, *Phys. Rev. B* **51**, 6773 (1995).
- ¹⁴B. Sadigh and V. Ozoliņš (unpublished); B. Sadigh, Ph.D. thesis, Royal Institute of Technology, Sweden, 1997. We use the optimization procedure of A. M. Rappe *et al.*, *Phys. Rev. B* **41**, 1227 (1990) and include multiple projectors for *s*- and *p*-angular momenta as suggested by P. Blöchl, *ibid.* **41**, 5414 (1990); D. Vanderbilt, *ibid.* **41**, 7892 (1990).
- ¹⁵X. W. Wang, B. N. Harmon, Y. Chen, K.-M. Ho, and C. Stassis, *Phys. Rev. B* **33**, 3851 (1986).
- ¹⁶H. J. Monkhorst and J. D. Pack, *Phys. Rev. B* **13**, 5188 (1976).
- ¹⁷Higher and lower temperature calculations show that the unstable phonon modes in these bcc metals are weakly stabilized with increasing electronic temperature [$\sim 0.6 \times 10^{-3}(\text{THz})^2/\text{K}$ for the $L[\frac{5}{8}\frac{5}{8}\frac{5}{8}]$ mode in Hf] but the stable phonons are not much affected.
- ¹⁸P. Blaha, K. Schwarz, P. Dufek, and R. Augustyn, WIEN95, Technical University of Vienna, 1995. [Improved and updated Unix version of the original copyrighted WIEN code, which was published in P. Blaha, K. Schwarz, P. Sorantin, and S. B. Trickey, *Comput. Phys. Commun.* **59**, 399 (1990).]
- ¹⁹V. L. Moruzzi, J. F. Janak, and A. R. Williams, *Calculated Electronic Properties of Metals* (Pergamon, New York, 1978).
- ²⁰A. T. Paxton, M. Methfessel, and H. M. Polatoglou, *Phys. Rev. B* **41**, 8127 (1990).
- ²¹N. Wakabayashi, S. K. Sinha, and F. H. Spedding, *Phys. Rev. B* **4**, 2398 (1971).
- ²²C. Stassis, D. Arch, and B. N. Harmon, *Phys. Rev. B* **19**, 181 (1979).
- ²³C. Stassis, D. Arch, O. D. McMasters, and B. N. Harmon, *Phys. Rev. B* **24**, 730 (1981).
- ²⁴T. Kraft, P. M. Marcus, M. Methfessel, and M. Scheffler, *Phys. Rev. B* **48**, 5886 (1993).
- ²⁵K.-M. Ho, C. L. Fu, and B. N. Harmon, *Phys. Rev. B* **29**, 1575 (1984).
- ²⁶M. Ekman, B. Sadigh, K. Einarsson, and P. Blaha, *Phys. Rev. B* **58**, 5296 (1998).
- ²⁷W. A. Bassett and E. Huang, *Science* **238**, 780 (1987).
- ²⁸Y. Chen, K. M. Ho, and B. N. Harmon, *Phys. Rev. B* **37**, 283 (1988).
- ²⁹K. Einarsson, B. Sadigh, G. Grimvall, and V. Ozoliņš, *Phys. Rev. Lett.* **79**, 2073 (1997).
- ³⁰R. J. Gooding, Y. Y. Te, C. T. Chan, K. M. Ho, and B. N. Harmon, *Phys. Rev. B* **43**, 13 626 (1991).
- ³¹V. G. Vaks, M. I. Katsnelson, V. G. Koreshkov, A. I. Likhentstein, O. E. Parfenov, V. F. Skok, V. A. Sukhoparov, A. V. Trefilov, and A. A. Chernyshov, *J. Phys.: Condens. Matter* **1**, 5319 (1989).
- ³²J. M. Sanchez, D. de Fontaine, *Phys. Rev. Lett.* **35**, 227 (1975).
- ³³B. M. Powell, A. D. B. Woods, and P. Martel, *Neutron Inelastic Scattering* (IAEA, Vienna, 1972), p. 43.
- ³⁴C. M. Varma and W. Weber, *Phys. Rev. B* **19**, 6142 (1979).